Pergamon

*Int. J. Heat Mass Transfer.* Vol. 39, No. 13, pp. 2831–2842, 1996

0017-9310/96 $15.00+0.00

0017-9310(95)00354-1

# Natural convection of non-Newtonian fluids along a wavy vertical plate including the magnetic field effect

YUE-TZU YANG, CHA'O-KUANG CHEN and MONG-TUNG LIN

Department of Mechanical Engineering, National Cheng Kung University, Tainan, Taiwan 701, Republic of China

(*Received* 17 *November* 1994)

**Abstract**—A Prandtl transformation method is applied to study the natural convection of non-Newtonian fluids along a wavy vertical plate in the presence of a magnetic field. A simple transformation is proposed, to transform the governing equations into the boundary layer equations, and solved numerically by the cubic spline approximation. A simple coordinate transformation is employed to transform the complex wavy surface to a vertical flat plate for a constant wall temperature by the numerical method. The effects of the magnetic field parameter, the wavy geometry and the non-Newtonian nature of the fluids on the flow characteristics and heat transfer are discussed in detail. It is found that the action of the magnetic field is to decelerate the flow, thus decreasing the Nusselt number. Copyright © 1996 Elsevier Science Ltd.

## INTRODUCTION

The laminar natural convection of a non-Newtonian fluid has been presented by many investigators because of its considerable practical applications. Since most of the non-Newtonian fluids are highly viscous and have large Prandtl number, similarity solutions have been obtained for such a fluid under various thermal boundary conditions [1–4]. The comparisons of the experimental data of Reilly *et al.* [5] and Dale and Emery [6] and the similarity results of Acrivos [1] and Chen [4] were good. A review of this subject was given by Shenoy and Mashelkar [7]. Natural convection of non-Newtonian fluids over an external surface was reported by Som and Chen [8], Kleinstreuer *et al.* [9], and Huang *et al.* [10]. All the previous analyses and experimental studies are available for different heating conditions for various kinds of geometries and for a variety of fluids. However, very few studies have been carried out which demonstrate the effects of complex geometries on natural convection such as a wavy surface, which is frequently used in finned heat exchangers and heat transfer enhancement devices. Yao [11] proposed a simple transformation to transform a complex geometry into a simple shape for which the equations of natural convection can be solved by a numerical finite difference method. The numerical results showed the frequency of the local heat transfer rate is twice that of the wavy surface. The steady-state laminar natural convection heat transfer of power-law non-Newtonian fluids along a wavy vertical plate was investigated by Kin and Chen [12] with a transformation method. The effects of Prandtl number, the dimensionless amplitude of the wavy plate and non-Newtonian flow index were examined in detail. All these analyses and experimental studies considered only a flat plate or simple two-dimensional bodies, and little has been done on non-Newtonian fluid heat transfer from a wavy surface imposed on a magnetic field. The action of a magnetic field on the fluid has many practical applications, e.g. metals processing industry, including the control of liquid metals in continuous casting processes, plasma welding, nuclear industry and many others. Mathematical modeling of the magnetohydrodynamics problems is particularly desirable.

In this present study the steady-state laminar convection heat transfer of power-law non-Newtonian fluid along a wavy vertical plate under the effect of magnetic field is studied. The results of dimensionless velocity fields, temperature profiles and heat transfer are obtained for this considered case. The effects of the wavy geometry and the non-Newtonian nature of the fluids on the flow and heat transfer characteristics are examined in detail.

## ANALYSIS

*Electromagnetic concepts*

It is well-known that an electrical conductor moving in a magnetic field generates an electromotive force (e.m.f.) which is proportional to its speed of motion and the magnetic field's strength, $H$. The fluid has to be electrically conducting as in the case of liquid metals or gases. The field of magnetohydrodynamics is complex for it involves the solution of both the Navier–Stokes equations characterizing fluid flow and Maxwell's equations for the magnetic field. In magnetofluidmechanics Maxwell's equations are presented as follows:

## NOMENCLATURE

| | |
|---|---|
| $B$ | magnetic flux density |
| $C_p$ | specific heat |
| $P$ | electric displacement flux |
| $E$ | electric field intensity |
| $Ec$ | Eckert number |
| $Gr$ | Grashof number |
| $H$ | magnetic field strength |
| $J$ | current density |
| $K$ | thermal conductively |
| $M_{gr}$ | $Mg^2 N_{gr}^{-1/2(2-n)}$ |
| $Nu$ | Nusselt number |
| $N_{gr}$ | generalized Grashof number |
| $P$ | Pressure |
| $Pr$ | Prandtl number |
| $N_{pr}$ | generalized Prandtl number |
| $T$ | temperature |
| $t$ | time |
| $u, v$ | velocity components in $(x, y)$ directions |
| $^*U, V$ | dimensionless velocity components |
| $x, y$ | coordinates |
| $X, Y$ | dimensionless coordinates. |

Greek symbols

| | |
|---|---|
| $\alpha$ | amplitude of wave |
| $\beta$ | thermal expansion coefficient |
| $\mu$ | viscosity |
| $\mu_e$ | magnetic permeability |
| $\delta$ | surface geometry function |
| $\rho$ | density |
| $\sigma$ | electrical conductivity |
| $\tau$ | dimensionless time |
| $\theta$ | dimensionless temperature. |

Superscripts

| | |
|---|---|
| $-$ | dimensionless quantity |
| $'$ | derivative with respect to $x$. |

Subscripts

| | |
|---|---|
| w | wall |
| $\infty$ | free stream. |

$$\nabla \cdot B = 0 \tag{1}$$

$$\nabla \cdot D = 0 \tag{2}$$

$$\nabla \times H = J \tag{3}$$

$$\nabla \times E = -\frac{\partial B}{\partial t}. \tag{4}$$

The magnetic flux density $B$ is expressed by

$$B = \mu_e H \tag{5}$$

$$D = \varepsilon E \tag{6}$$

where $J$ is the current density, $\mu_e$ is the magnetic permeability and $E$ is the electric field intensity. By Ohm's law, the total current flow can be defined as

$$J = \sigma(E + V \times B) \tag{7}$$

where $\sigma$ = electrical conductivity.

By combining the above equations, with $H$ replaced by $B/\mu_e$, we have

$$\frac{\partial B}{\partial t} = \nabla \times (V \times B) + \nu_m \nabla^2 B \tag{8}$$

where $\nu_m = 1/\sigma\mu_e$

In the momentum equation, we have to include the electromagnetic force, $F_m$, which is

$$F_m = J \times B = \sigma(V \times B) \times B. \tag{9}$$

*Governing equations*

Consider a steady-state natural convection of non-Newtonian fluids along a wavy vertical plate imposed on a magnetic field. The physical model and coordinate system is shown in Fig. 1, where $(u, v)$ are velocity components in the $(x, y)$ directions. The surface of the plate is described by $y = \delta(x)$, where $\delta(x)$ is an arbitrary geometric function. The temperature of the plate is held at a constant value $T_w$, which is higher than the ambient temperature $T_\infty$. In the present study, the electrically conducting fluids are assumed to be non-Newtonian fluids, with two-dimensional incompressible flow, and the magnetic Reynolds number is small. The properties of the fluids are

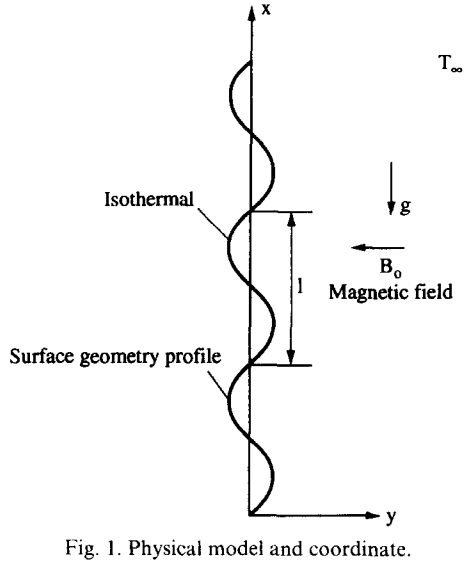


Fig. 1. Physical model and coordinate.

assumed to be constant, except for the density in the buoyancy force term. A magnetic field with a constant magnetic flux density, $B_0$, is applied. In magneto-fluid mechanics, fluid motion is governed by the laws of conservation of mass, momentum and energy. The equation of continuity remains unchanged. The momentum and energy equations must be modified from Maxwell's field equation and Ohm's law. Based on the above assumptions, the governing equations of continuity, momentum and energy for the steady-state natural convection of non-Newtonian fluids along a wavy vertical plate, including the magnetic field effect, are

$$\frac{\partial u}{\partial x}+\frac{\partial v}{\partial y}=0 \tag{10}$$

$$\frac{\partial u}{\partial t}+u\frac{\partial u}{\partial x}+v\frac{\partial u}{\partial y}=-\frac{1}{\rho}\frac{\partial P}{\partial x}-\frac{1}{\rho}\left(\frac{\partial \tau_{xx}}{\partial x}+\frac{\partial \tau_{xy}}{\partial y}\right)+g\beta(T-T_\infty)-\frac{\sigma B_0^2}{\rho}u \tag{11a}$$

$$\frac{\partial v}{\partial t}+u\frac{\partial v}{\partial x}+v\frac{\partial v}{\partial y}=-\frac{1}{\rho}\frac{\partial P}{\partial y}-\frac{1}{\rho}\left(\frac{\partial \tau_{yx}}{\partial x}+\frac{\partial \tau_{yy}}{\partial y}\right) \tag{11b}$$

$$\frac{\partial T}{\partial t}+u\frac{\partial T}{\partial x}+v\frac{\partial T}{\partial y}=\alpha\left(\frac{\partial^2 T}{\partial x^2}+\frac{\partial^2 T}{\partial y^2}\right)+\frac{\sigma B_0^2}{\rho C_p}u^2. \tag{12}$$

*Prandtl's transposition theorem*

The first step is to transform the irregular wavy surface into a flat surface by use of Prandtl's transposition theorem, Yao [13]. The theorem is that the flow is displaced by the amount of the vertical displacement of an irregular solid surface, and the vertical component of the velocity is adjusted according to the slope of the surface. The form of the boundary-layer equations is invariant under the transformation, and the surface conditions can be applied on a transformed flat surface. This allows the boundary conditions to be easily incorporated into any numerical method. In order to transform the above governing equations, the following dimensionless quantities are introduced:

$$\bar{x}=\frac{x}{l} \tag{13a}$$

$$\bar{y}=\frac{y-\delta}{l}N_{gr}^{1/2(n+1)} \tag{13b}$$

$$\bar{u}=\frac{u}{\sqrt{lg\beta\Delta T}}=\frac{u}{u_\infty} \tag{13c}$$

$$\bar{v}=\frac{v-\delta' u}{\sqrt{lg\beta\Delta T}}N_{gr}^{1/2(n+1)}=\frac{v-\delta' u}{u_\infty}N_{gr}^{1/2(n+1)} \tag{13d}$$

$$\delta'=\frac{d\delta}{dx}=\frac{d\bar{\delta}}{d\bar{x}}\quad \bar{\delta}=\frac{\delta}{l} \tag{13e}$$

$$\bar{P}=\frac{P}{\rho lg\beta\Delta T}=\frac{P}{\rho u_\infty^2} \tag{13f}$$

$$\theta=\frac{T-T_\infty}{T_w-T_\infty} \tag{13g}$$

$$N_{gr}=\frac{\rho^2 l^{n+2}[g\beta\Delta T]^{2-n}}{m^2} \tag{13h}$$

$$N_{pr}=\frac{\rho C_p}{k}\left(\frac{m}{\rho}\right)^{2/1+n}(l)^{(1-n)/(1+n)}[lg\beta\Delta T]^{3(n-1)/2(1+n)} \tag{13i}$$

where $N_{gr}$ and $N_{pr}$ are the generalized Grashof number and the generalized Prandtl number, respectively. By use of equation (10a), we transform the wavy surface into a flat surface. Neglecting the small order in $N_{gr}$, the governing equations are transformed to

$$\frac{\partial \bar{u}}{\partial \bar{x}}+\frac{\partial \bar{v}}{\partial \bar{y}}=0 \tag{14}$$

$$\frac{\partial \bar{u}}{\partial \bar{t}}+\bar{u}\frac{\partial \bar{u}}{\partial \bar{x}}+\bar{v}\frac{\partial \bar{u}}{\partial \bar{y}}=-\frac{\partial \bar{p}}{\partial \bar{x}}+\delta' N_{gr}^{1/2(n+1)}\frac{\partial \bar{p}}{\partial \bar{y}}+\theta+(1+\delta'^2)\frac{\partial}{\partial \bar{y}}\left(\left|\frac{\partial \bar{u}}{\partial \bar{y}}\right|^{n-1}\frac{\partial \bar{u}}{\partial \bar{y}}\right)-M_g^2 N_{gr}^{-1/2(2-n)}\bar{u} \tag{15}$$

$$\delta''\bar{u}^2+\delta'\theta=\delta'\frac{\partial \bar{p}}{\partial \bar{x}}-(1+\delta'^2)N_{gr}^{1/2(n+1)}\frac{\partial \bar{p}}{\partial \bar{y}}+\delta' M g^2 N_{gr}^{-1/2(2-n)}\bar{u} \tag{16}$$

$$\frac{\partial \theta}{\partial \bar{t}}+\bar{u}\frac{\partial \theta}{\partial \bar{x}}+\bar{v}\frac{\partial \theta}{\partial \bar{y}}=\frac{1}{Pr}(1+\delta'^2)\frac{\partial^2 \theta}{\partial \bar{y}^2}+M^2 E_c G_r^{-1/2}\bar{u}^2 \tag{17}$$

where

$$M_g^2=\frac{\sigma B_0^2 \rho^{1/2-n} l^{2/2-n}}{\rho m^{1/2-n}}\quad M^2=\frac{\sigma B_0^2 l^2}{\rho\nu}. \tag{18}$$

The transformed momentum equations (15) and (16) can be combined into one equation by neglecting the pressure gradient, and so, we have

$$\frac{n+1}{n}U+[2(n+1)X]\frac{\partial U}{\partial X}-Y\frac{\partial U}{\partial Y}+[2(n+1)X]^{(n-1)(2n+1)/2n(n+1)}\frac{\partial V}{\partial Y}=0 \tag{19}$$

$$\frac{\partial U}{\partial \tau}+[2(n+1)X]^{1/n}U\frac{\partial U}{\partial X}+\{[2(n+1)X]^{(1-n)/2n(n+1)}V-[2(n+1)X]^{(1-n)/n}UY\}\frac{\partial U}{\partial Y}$$

$$= (1+\delta'^2)^{-1}\{\theta - M_g^2 N_{gr}^{-1/2(2-n)}[2(n+1)X]^{1/2n}U\}$$

$$-\left\{\frac{n+1}{n}[2(n+1)X]^{(1-n)/n} + \frac{1}{(1+\delta'^2)}\delta'\delta''[2(n+1)X]^{1/n}\right\}U^2$$

$$+(1+\delta'^2)\frac{\partial}{\partial Y}\left(\left|\frac{\partial U}{\partial Y}\right|^{n-1}\frac{\partial U}{\partial Y}\right) \quad (20)$$

$$[2(n+1)X]^{(n-1)/2n(n+1)}\frac{\partial\theta}{\partial\tau} + [2(n+1)X]^{(3n+1)/2n(n+1)}U\frac{\partial\theta}{\partial X} + \{V-[2(n+1)X]^{(1+2n)(1-n)/2n(n+1)}UY\}\frac{\partial\theta}{\partial Y}$$

$$= Pr^{-1}(1+\delta'^2)\frac{\partial^2\theta}{\partial Y^2} + M^2 Ec\, Gr^{-1/2}[2(n+1)X]^{(2n+1)/n(n+1)}U^2 \quad (21)$$

where

$$X = \bar{x} \quad (22a)$$

$$Y = \bar{y}/[2(n+1)X]^{1/2(n+1)} \quad (22b)$$

$$U = \bar{u}/[2(n+1)X]^{1/2n} \quad (22c)$$

$$V = [2(n+1)X]^{1/2(n+1)}\bar{v} \quad (22d)$$

$$\theta = \theta \quad \tau = \bar{t}/[2(n+1)X]^{1/2n} \quad (22e)$$

with the corresponding boundary conditions,

$$\left.\begin{array}{l} X = 0 \quad U = \theta = 0 \\ Y = 0 \quad U = V = 0 \quad \theta = 1 \end{array}\right\} \quad (23)$$

$$Y \to \infty \quad U = \theta = 0. \quad (24)$$

The local Nusselt number and the averaged Nusselt number can be determined by using Newton's cooling law and Fourier's law,

$$Nu_x = -[N_{gr}/2(n+1)X]^{1/2(n+1)}(1+\delta'^2)^{1/2}\left.\frac{\partial\theta}{\partial Y}\right|_{Y=0} \quad (25)$$

$$\overline{Nu_x} = -\frac{1}{S}\int_0^X [N_{gr}/2(n+1)X]^{1/2(n+1)} \times (1+\delta'^2)\left.\frac{\partial\theta}{\partial Y}\right|_{Y=0} dX \quad (26)$$

where

$$S = \int_0^X [1+\delta'^2]^{1/2}\, dx.$$

## NUMERICAL ANALYSIS

The governing equations with the corresponding constant temperature boundary condition were solved by using the cubic spline approximation method, Rubin and Graves [14]. The SADI procedure was applied to perform the numerical computation. Using the spline formulation, the natural convection boundary layer equation is written in the following form:

$$\Phi_{ij}^{n+1} = F_{ij} + G_{ij}(m\Phi)_{ij}^{n+1} + S_{ij}(M\Phi)_{ij}^{n+1} \quad (27)$$

where

$$(m\Phi)_{ij}^{n+1} = \left(\frac{\partial\Phi}{\partial Y}\right)_{ij}^{n+1} \quad (28)$$

$$(M\Phi)_{ij}^{n+1} = \left(\frac{\partial^2\Phi}{\partial Y^2}\right)_{ij}^{n+1} \quad (29)$$

and the functions of $F$, $G$ and $S$ are shown in Table 1.

In this study, the iteration process is continued until the convergence criterion, is achieved

$$\left|\frac{\Phi_{ij}^{n+1} - \Phi_{ij}^{n}}{\Phi_{max}^{n}}\right| < 10^{-4}. \quad (30)$$

## RESULTS AND DISCUSSION

In order to verify the numerical accuracy of the solution, numerical results were first obtained for the case of a Newtonian fluid ($n = 1.0$) with constant wall temperature and compared to those reported by Yao [11], as shown in Table 2. Table 2 shows a comparison of the present calculation of local Nusselt number with different grid number. The calculation solutions appear to be independent of the grid number of the $X$-axis. The results agree well with grid number of $y = 61$. It also demonstrates that cubic spline approximation saves much CPU time. The effects of the magnetic field parameter $M_{gr}$, the wavy geometry $\alpha$ and the power law index $n$ on flow characteristics and heat transfer have been studied.

Figure 2(a–c) represents the axial velocity distribution with dimensionless amplitude of wave $\alpha = 0.0$, 0.1 and 0.2, $n = 1.2$, 1.0 and 0.6 with $Pr = 10.0$. The results agree with that obtained by Kim and Chen [12] for the case of a power law fluid in the absence of a magnetic field. With the increase of $n$, the maximum $U$ increases, but the velocity boundary layer becomes thinner. The effect of the dimensionless wave amplitude $\alpha$ on the velocity distribution is presented, as $\alpha$ increased the maximum $U$ decreases and the velocity boundary layer becomes slightly thicker. The effect of $n$ on the temperature distribution with $\alpha = 0.0$, 0.1 and 0.2, $Pr = 10.0$ is presented in Figs. 3–5. The dilatant fluid $n = 1.2$ has a thinner thermal boundary layer, but larger wall temperature gradient that the pseudoplastic fluid ($n = 0.6$). For a given fluid, the increase of $\alpha$ tends to

Table 1. Function of $F$, $G$ and $S$

$$F_{ij}^{\theta} \qquad \theta_{ij}^{k}-[2(n+1)X_i]^{1/n}U_{ij}^{k}\frac{\theta_{ij}^{k}-\theta_{i-1,j}^{k}}{X_i-X_{i-1}}\Delta\tau$$

$$G_{ij}^{\theta} \qquad \left([2(n+1)X_i]^{1-n/n}U_{ij}^{k}Y_j-\frac{V_{ij}^{k}}{[2(n+1)X_i]^{(n-1)/2n(n+1)}}\right)\Delta\tau$$

$$S_{ij}^{\theta} \qquad \frac{1+\delta_i'^2}{Pr}\frac{\Delta\tau}{[2(n+1)X_i]^{(n-1)/2n(n+1)}}$$

$$F_{ij}^{U} \qquad \left(U_{ij}^{k}-[2(n+1)X_i]^{1-n/n}Y_jU_{ij}^{k}mU_{ij}^{k}\Delta\tau\right.$$

$$+\frac{\Delta\tau}{1+\delta_i'^2}(\theta_{ij}^{k}-Mg^2N_{gr}^{-1/2(2-n)}[2(n+1)X_i]^{1/2n}U_{ij}^{k})$$

$$-U_{ij}^{k2}\left(\frac{n+1}{n}[2(n+1)X_i]^{1-n/n}+\frac{\delta_i'\delta_i''}{1+\delta_i'^2}[2(n+1)X_i]^{1/n}\right)\Delta\tau$$

$$\left.-[2(n+1)X_i]^{1/n}U_{ij}^{k}\frac{U_{ij}^{k}-U_{i-1,j}^{k}}{X_i-X_{i-1}}\Delta\tau\right)\Big/(1-[2(n+1)X_i]^{1-n/n}Y_jmU_{ij}^{k}\Delta\tau)$$

$$G_{ij}^{U} \qquad \left([2(n+1)X_i]^{1-n/n}U_{ij}^{k}Y_j\Delta\tau-[2(n+1)X_i]^{(1-n)/2n(n+1)}V_{ij}^{k}\Delta\tau\right.$$

$$\left.+(1+\delta_i'^2)\frac{|mU_{ij}^{k}|^{n-1}-|mU_{i,j-1}^{k}|^{n-1}}{Y_j-Y_{j-1}}\Delta\tau\right)\Big/(1-[2(n+1)X_i]^{1-n/n}Y_jmU_{ij}^{k}\Delta\tau)$$

$$S_{ij}^{U} \qquad (1+\delta_i'^2)|mU_{ij}^{k}|^{n-1}\Delta\tau/(1-[2(n+1)X_i]^{1-n/n}Y_jmU_{ij}^{k}\Delta\tau)$$

Table 2. Comparison with the results of Yao [11] for different grid number

| Grid number | 41 * 41 | 41 * 46 | 41 * 81 | 41 * 101 |
|---|---|---|---|---|
| Local Nusselt number | 0.5693 | 0.5672 | 0.5662 | 0.5656 |
| Grid number | 61 * 41 | 61 * 61 | 61 * 81 | 61 * 101 |
| Local Nusselt number | 0.5693 | 0.5673 | 0.5662 | 0.5657 |
| Grid number | 81 * 41 | 81 * 61 | 81 * 81 | 81 * 101 |
| Local Nusselt number | 0.5694 | 0.5673 | 0.5663 | 0.5657 |
| Grid number | 101 * 41 | 101 * 61 | 101 * 81 | 101 * 101 |
| Local Nusselt number | 0.5694 | 0.5674 | 0.5664 | 0.5658 |
| Yao [11] Local Nusselt number | 161 * 501 0.5671 ($X = 2.0$) $Pr = 1.0$, $M_{gr} = 0.0$ $\alpha = 0.0$, $n = 1.0$ $X = 4.0$, $Y = 10.0$ | | | |

thicken the thermal boundary layer and retard the heat transfer rate at the wall surface. The present calculations in the absence of a magnetic field are in good agreement with the results of Yao [11] and Kim and Chen [12]. Therefore, the present results should have a relatively high degree of accuracy, although no available exact results can be compared with the present results when $M_{gr} = 0.0$.

The influence of the wave amplitude on the flow and heat transfer characteristics is examined as shown in Figs. 6–8 with constant magnetic strength $M_{gr} = 1.0$ for $Pr = 0.1$ and $n = 1.2$ and 0.8. Increasing the wave amplitude $\alpha$ from 0 to 0.2 will decrease the axial velocity and increase the variation of normal velocity. For a given fluid, the increase of $\alpha$ tends to thicken the velocity boundary layer and thermal boundary layer. The waviness of the plate reduces the local Nusselt number. The effect of magnetic field strength is presented in Figs. 9–11. As the magnetic field strength increases, as indicated by an increasing $M_{gr}$, the temperature of the fluid increases, but the velocity decreases. It also takes longer to reach the steady-state. Figures 12–14 display the effect of Prandtl number on the velocity, as well as the temperature distribution. With increasing Prandtl number, the axial velocity and temperature decrease.

The numerical results are presented for $\delta = \alpha\sin(2\pi x)$ to demonstrate the advantage of the transformation method. The velocity and temperature of the node, trough and crest are plotted for $\alpha = 0.1$ in Figs. 15–17. The node of the wave is at $x = 1.0$, while $x = 0.75$ is the trough and $x = 1.25$ is the crest. The velocity profile at the trough and the crest differs only slightly. It is clear that the boundary layer is thicker near the nodes than near the trough and the crest. The temperature gradient has to be corrected by the local curvature before the heat transfer rate can be calculated, since the $y$-direction is not normal to

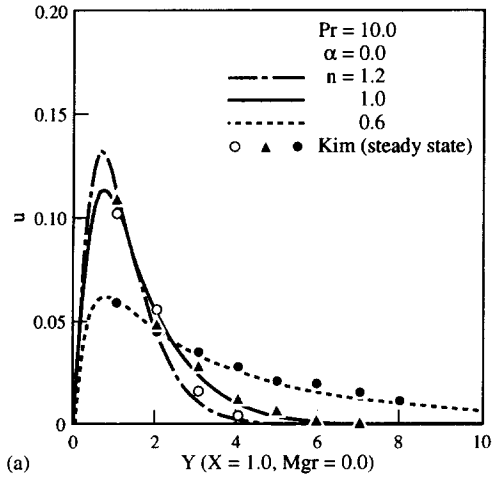


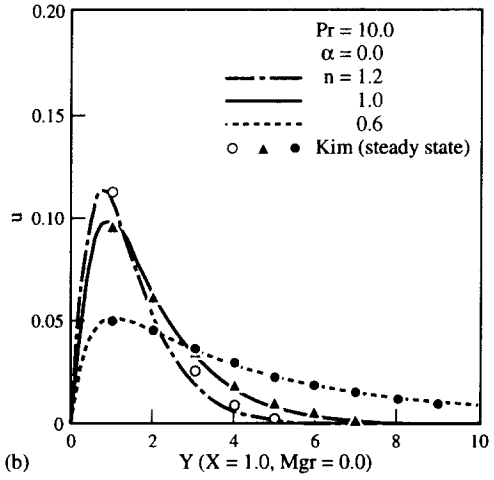


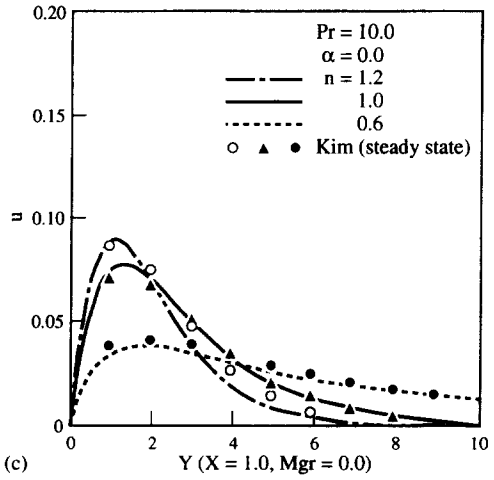


Fig. 2. (a) Dimensionless axial velocity distribution $\alpha = 0.0$, (b) dimensionless axial velocity distribution for $\alpha = 0.1$, (c) dimensionless axial velocity distribution for $\alpha = 0.2$.

the wavy surface. The averaged Nusselt number distribution for the case of a flat plate ($\alpha = 0$) and the wavy surfaces for $n = 1.2$ and $Pr = 0.1$ and 10 is shown in Fig. 18(a, b). It is seen that the waviness of the plate reduces the averaged local Nusselt number.

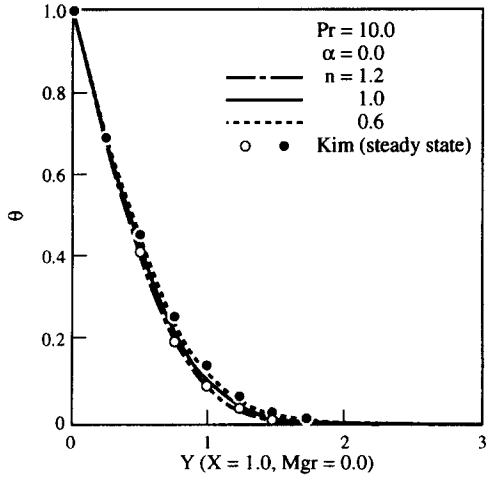


Fig. 3. Dimensionless temperature distribution at $X = 1$ and $\alpha = 0.0$.

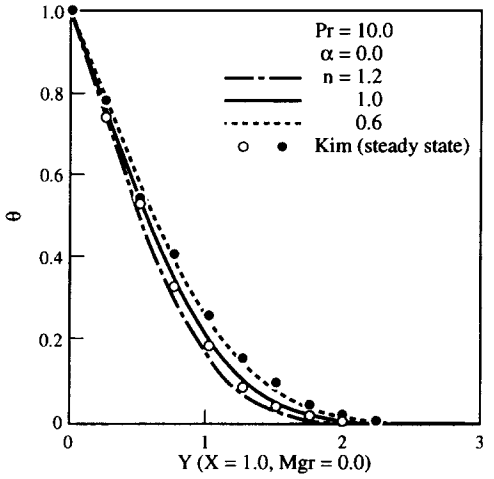


Fig. 4. Dimensionless temperature distributed at $X = 1$ and $\alpha = 0.1$.

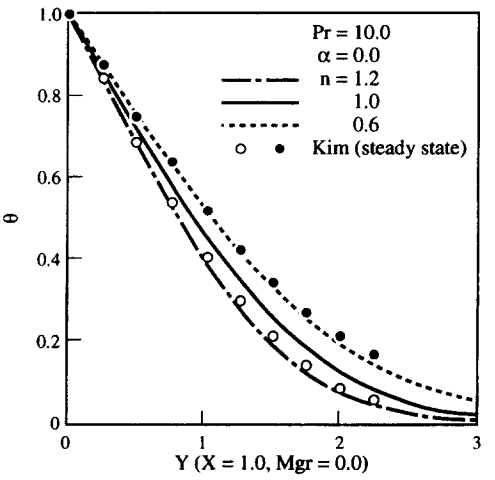


Fig. 5. Dimensionless temperature distribution at $X = 1$ and $\alpha = 0.2$.

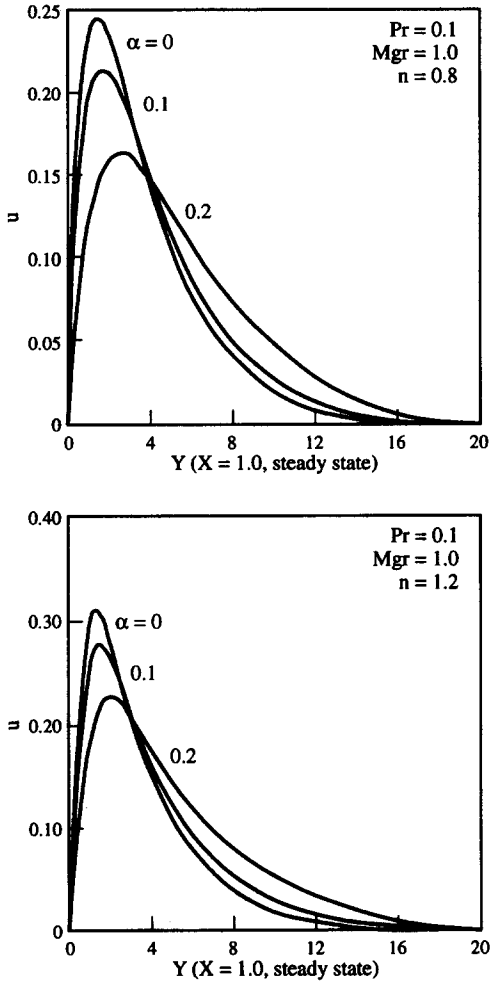


Fig. 6. Axial velocity distribution for different wave amplitude ($n$ = 1.2 and 0.8).

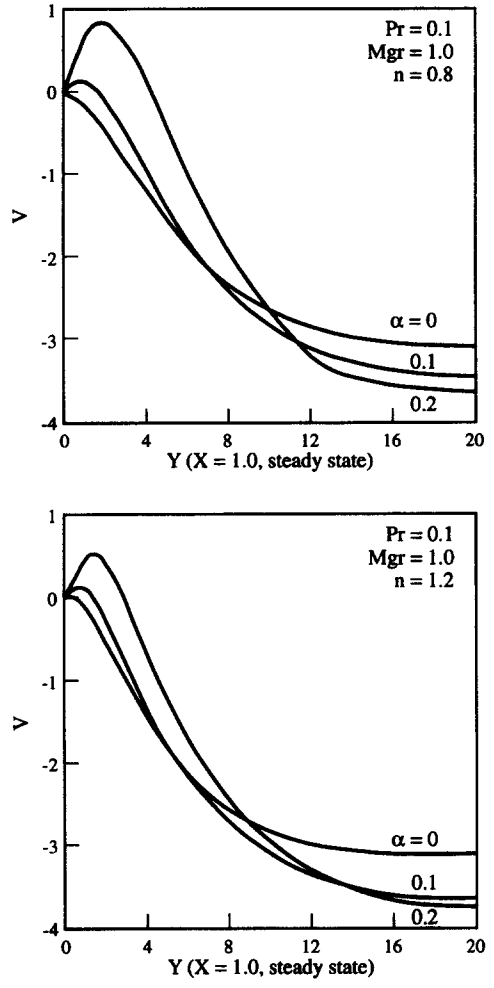


Fig. 7. Normal velocity distribution for different wave amplitude ($n$ = 1.2 and 0.8).

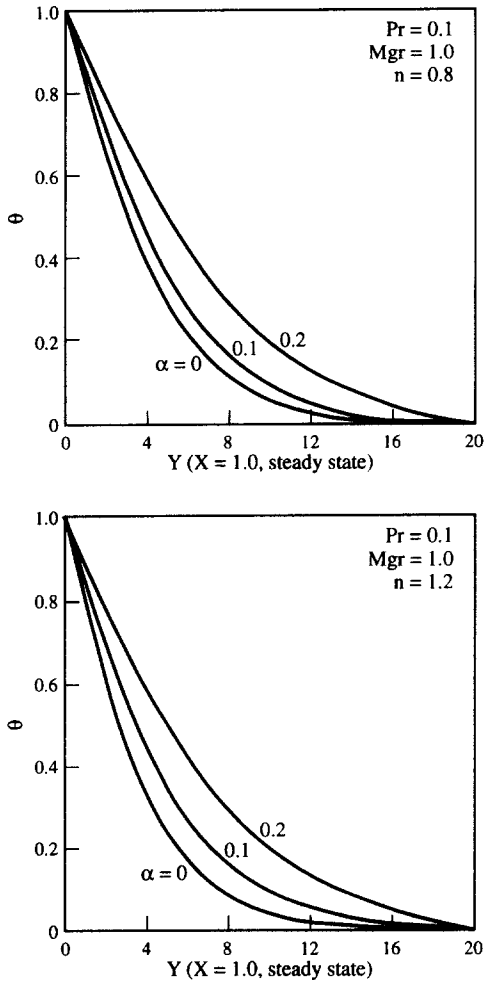


Fig. 8. Dimensionless temperature distribution for different wave amplitude ($n = 1.2$ and 0.8).

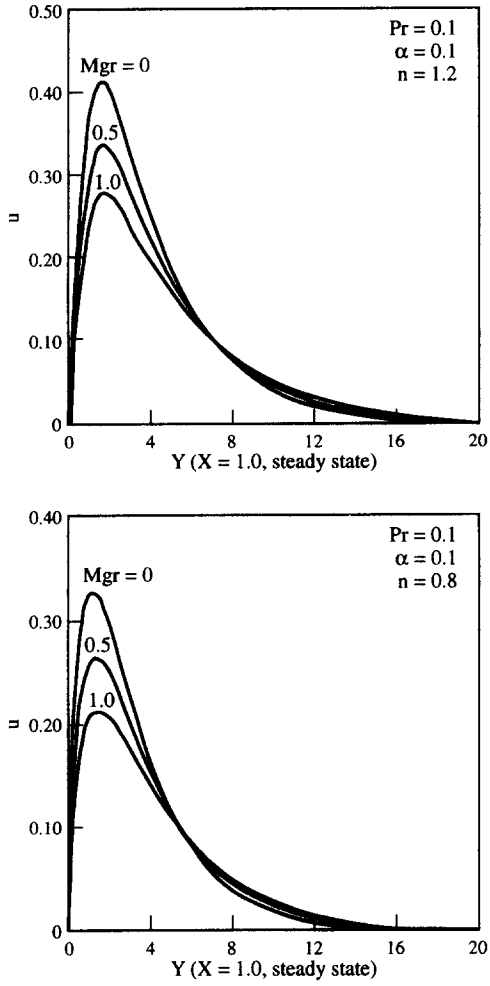


Fig. 9. Axial velocity distribution for different magnetic strength ($Pr = 0.1$, $n = 1.2$ and 0.8).

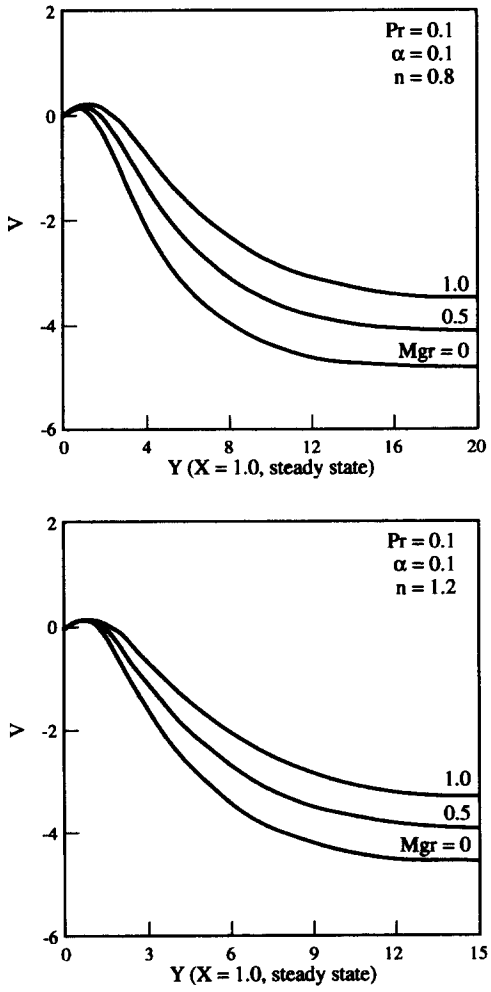


Fig. 10. Normal velocity distribution for different magnetic strength ($Pr = 0.1$, $n = 1.2$ and 0.8).

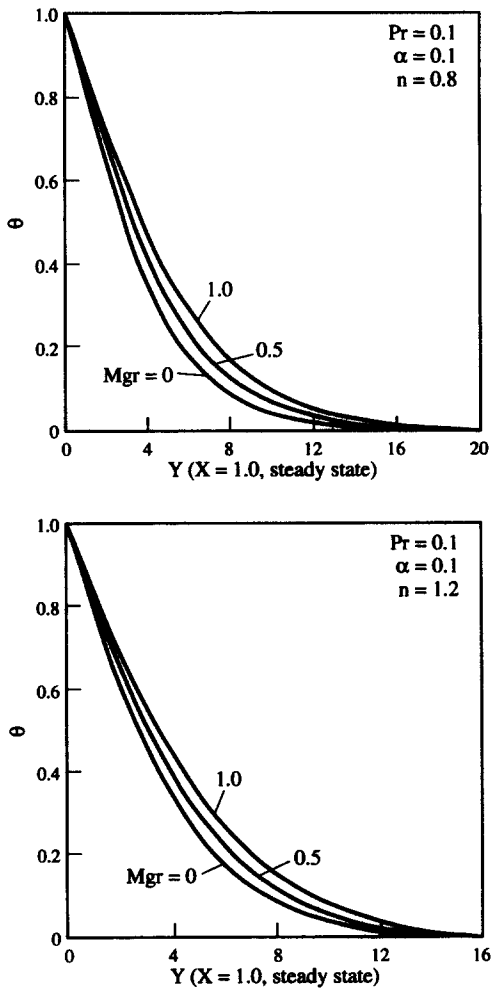


Fig. 11. Dimensionless temperature distribution for different magnetic strength ($Pr = 0.1$, $n = 1.2$ and 0.8).

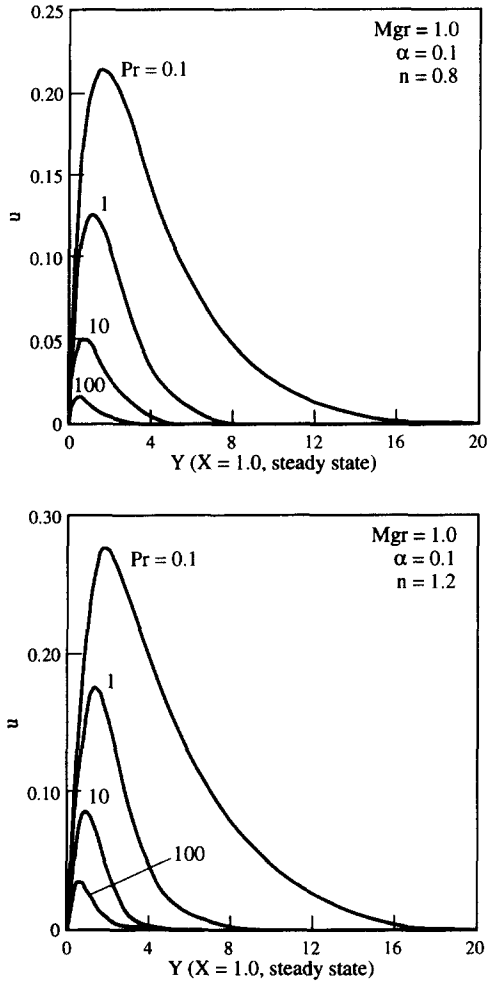


Fig. 12. Axial velocity distribution for different Prandtl number ($n$ = 1.2 and 0.8).

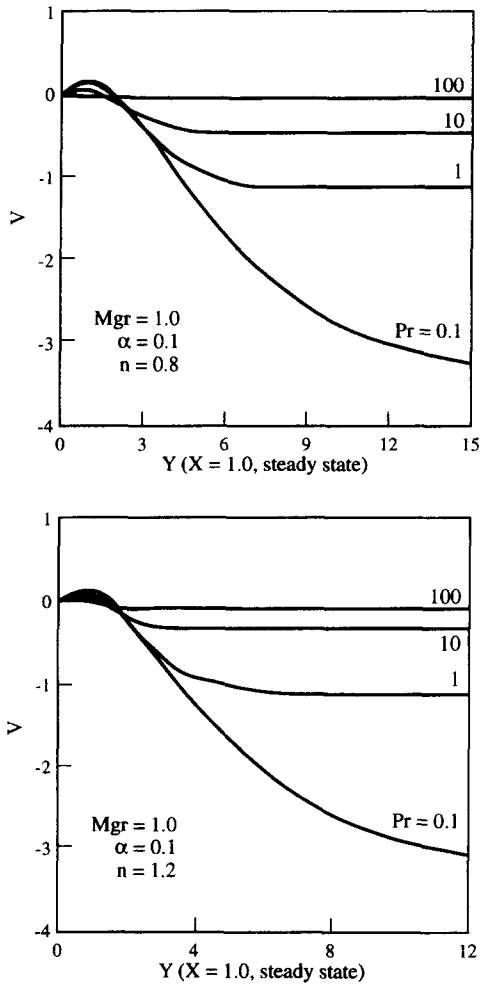


Fig. 13. Normal velocity distribution for different Prandtl number ($n$ = 1.2 and 0.8).

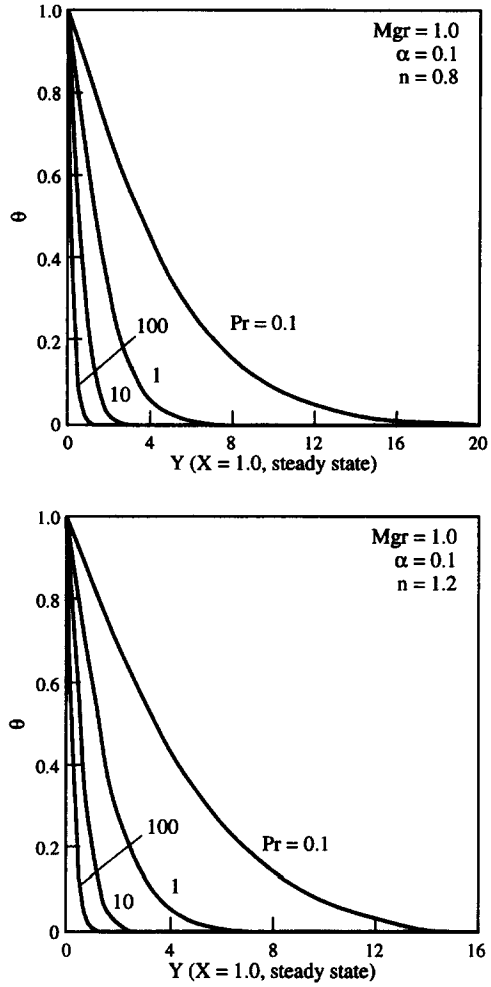


Fig. 14. Dimensionless temperature distribution for different Prandtl number ($n = 1.2$ and 0.8).

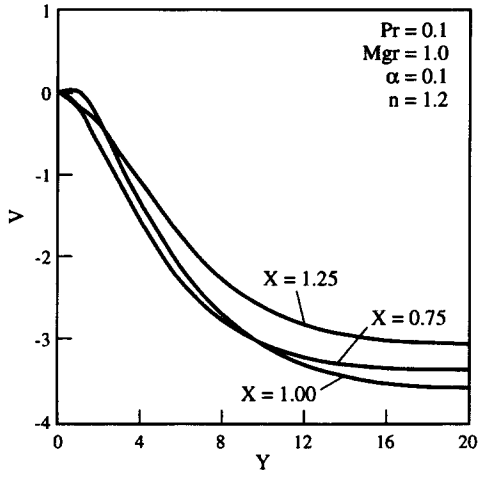


Fig. 16. Normal velocity profile of node, trough and crest.

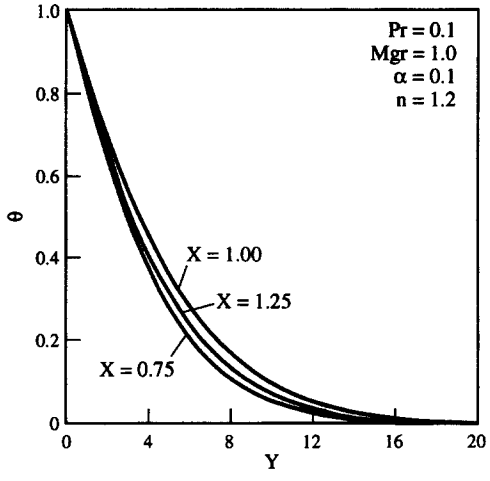


Fig. 17. Temperature distribution.

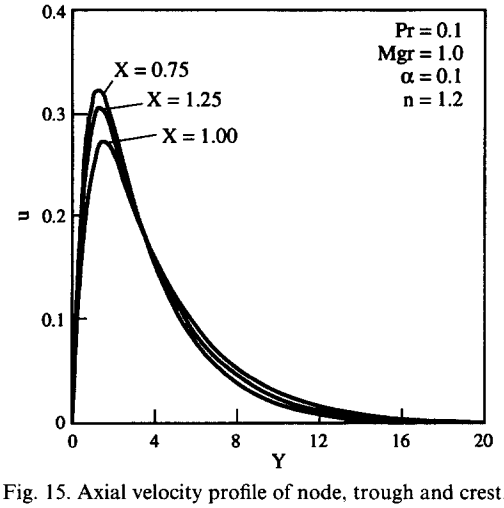


Fig. 15. Axial velocity profile of node, trough and crest.

## CONCLUSIONS

The main conclusions of this study are:

(1) The use of Prandtl transformation method can transform the Navier–Stokes equations into a boundary layer equation. It also can solve the problem due to the complexity of the boundary.

(2) The present prediction demonstrates that this problem can be solved effectively by using cubic spline approximation.

(3) The averaged heat transfer coefficient for a wavy surface is smaller than that of the corresponding flat plate. The total heat transfer rate for a wavy surface is about the same as that of a flat plate for considering larger heat transfer area.

(4) The temperature of flow increases, but decreases the velocity in the presence of magnetic field. The magnetic field can therefore be used to control the flow characteristics.

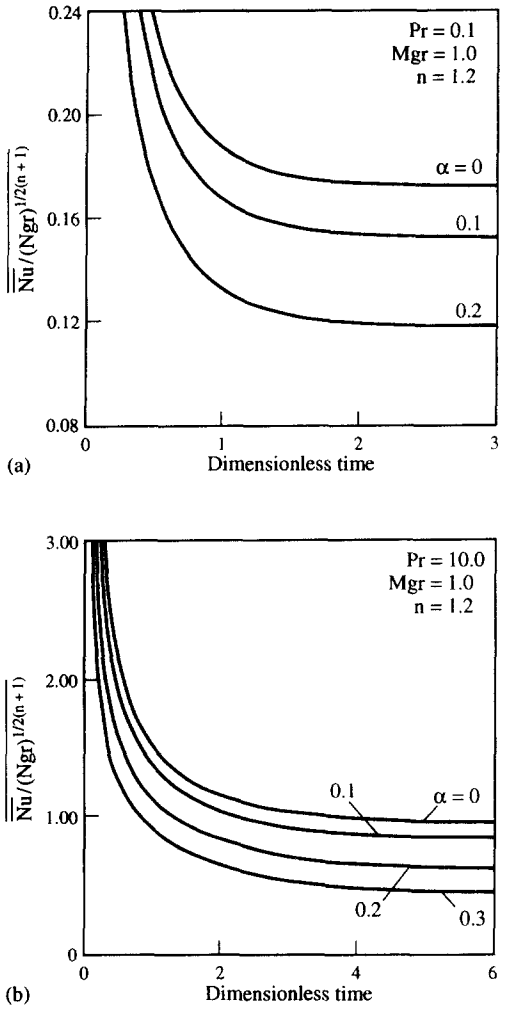


Fig. 18. Averaged Nusselt number distribution for (a) $Pr = 0.1$, (b) $Pr = 10$.

## REFERENCES

1. A. Acrivos, A theoretical analysis of laminar natural convection heat transfer to non-Newtonian fluids, *A.I.Ch.E. J.* **6,** 584–590 (1960).
2. S. Y. Lee and W. F. Ames, Similarity solutions for non-Newtonian fluids, *A.I.Ch.E. J.* **12,** 700–708 (1966).
3. Na, T. Y. and Hansen, A. G., Possible similarity solutions of the laminar natural convection flow of non-Newtonian fluids, *Int. J. Heat Mass Transfer*, **9,** 261 262 (1966).
4. J. L. S. Chen, Natural convection of power-law fluids from a vertical plate with uniform surface heat flux, *Heat Transfer* 1974, *5th Int. Heat Transfer Conf.*, Science Council of Japan, Vol. 3, pp. 39–43 (1974).
5. I. G. Reilly, C. Tien and M. Adelman, Experimental study of natural convection heat transfer from a vertical plate in a non-Newtonian fluid, *Can. J. Chem. Engng* **43,** 157–160 (1965).
6. J. D. Dale and A. F. Emery, The free convection of heat from a vertical plate to several non-Newtonian pseudo-plastic fluids, *J. Heat Transfer* **94,** 63–72 (1972).
7. A. V. Shenoy and R. A. Mashelkar, Thermal convection in non-Newtonian fluids, *Adv. Heat Transfer* **15,** 143–225 (1982).
8. A. Som and J. L. S. Chen, Free convection of non-isothermal two-dimensional bodies, *Int. J. Heat Mass Transfer* **27,** 791–794 (1984).
9. C. Kleinstreuer, T. Y. Wang and S. Haq, Natural convection heat transfer between a power-law fluid and a permeable isothermal vertical wall. In *Fundamentals of Convection in Non-Newtonian Fluids* (Edited by J. L. S. Chen, J. M. Ekmann and G. P. Peterson), HTD Vol. 79, pp. 25–31. (1987).
10. M. Huang, J. Huang, Y. Chou and Y. Chen, Effects of Prandtl number on free convection heat transfer from a vertical plate to a non-Newtonian fluid, *J. Heat Transfer* **111,** 189–191 (1989).
11. L. S. Yao, Natural convection along a vertical wavy surface, *J. Heat Transfer* **105,** 465–468 (1983).
12. Eunpil Kim and J. L. S. Chen, Natural convection of non-Newtonian fluids along a wavy vertical plate. In *Fundamentals of Heat Transfer in Non-Newtonian Fluids*, HTD Vol. 174. ASME (1991).
13. L. S. Yao, A note on Prandtl's transposition theorem, *J. Heat Transfer* **110,** 507–508 (1988).
14. S. G. Rubin and R. A. Graves, Viscous flow solution with a cubic spline approximation, *Comput. Fluids* **3,** 1 36 (1975).